Engineering Structures 101 (2015) 743–749

Contents lists available at ScienceDirect

Engineering Structures

journal homepage: www.elsevier.com/locate/engstruct

Joints and wood shear walls modelling II: Experimental tests and FE models under seismic loading

C. Boudaud [a], J. Humbert [b], J. Baroth [c,*], S. Hameury [d], L. Daudeville [c]

[a] LUNAM Univ., Groupe Ecole Superieure du Bois, Nantes, France
[b] Korea Forest Research Institute, Seoul, Republic of Korea
[c] UJF-Grenoble 1, Grenoble-INP, CNRS UMR 5521, 3SRLab, Grenoble F-38041, France
[d] Centre Scientifique et Technique du Bâtiment, Marne-la-Vallée, France

ARTICLE INFO

Article history:
Received 27 January 2014
Revised 17 September 2014
Accepted 21 October 2014
Available online 29 November 2014

Keywords:
Timber-framed structures
Shear walls
Finite element method
Seismic tests

ABSTRACT

This study presents a finite element (FE) model of timber-framed shear walls under seismic loading, which has been validated in Part I under quasi-static loading. In this paper, experimental shake table tests on shear walls are described and some examples of the obtained results are discussed. Then, the refined FE model predictions under dynamic loading are compared to the 11 shake table tests. The final objective of this study is to create a 3D model of timber-framed structures; thus, a simplified FE model is proposed to reproduce the refined FE model predictions at a reasonable computational cost. The calibration method of the simplified model uses the predictions of the refined FE model under quasi-static loading as input. The simplified model is then used for dynamic calculations and its predictions are confronted to the refined FE model ones, in order to validate its behaviour under dynamic loading. Eventually, an efficient method to build the walls of a timber-framed building by coupling simplified FE models is proposed.

1. Introduction

This paper is the second part of two companion papers that couples experimental and numerical studies with the objective of investigating timber-framed structures under seismic loading. The study focuses on shear wall behaviour and its modelling because shear walls are the structural elements that primarily contributes to the lateral resistance of timber-framed buildings. The proposed approach consists of building the constitutive behaviour of simplified finite elements (FE) models at the appropriate scale to predict the structural response at the larger scale. In Part I, a phenomenological model of joints with metal fasteners was proposed for a refined model of shear walls, and was calibrated using the test results performed on various joints (Panel-to-frame (P2F) nails, Frame-to-frame (F2F) nails, standard (E5®) or reinforced (AH) bracket-type 3D connectors provided by Simpson Strong-Tie®). More than 300 experimental tests were performed, more details can be found in Part I. This modelling approach on a smaller scale (from joint to shear wall behaviour) was validated based on the good agreement between the refined FE model predictions and the experimental results of shear wall behaviour under quasi-static loading.

Many previous studies have proposed constitutive models for joints and shear walls [11,21,25,18,19,14,16]. As many of them, the model proposed in Part I of this paper is based on user-defined parameters that are calibrated thanks to monotonic and hysteretic responses of joints or shear walls. The first part of these two companion papers also emphasised several points:

- The hysteretic constitutive model presented in Part I uses Bézier curves instead of exponential functions to assure strict analytical continuity, which is necessary to reproduce the nonlinear behaviour of all the joints with metal fasteners used in timber-framed structures (nails, 3D bracket-type connectors, punched metal plates). Thus, the model can describe asymmetric hysteresis loops.
- To account for the behavioural variability of joints with metal fasteners, 5 quasi-static reversed-cyclic tests were repeated for each configuration. The constitutive model was calibrated based on the average behaviour, which is less time consuming and provides similar results as averaging parameters calibrated from each test [25].
- Repeated quasi-static tests performed on different configurations of shear walls provide an important experimental database (14 tests) used to validate both the refined FE model of shear walls and the hysteretic constitutive model of joints.

* Corresponding author at: 3SR Laboratory, Domaine Universitaire, BP53, 38041 Grenoble Cedex 9, France.

E-mail addresses: clement.boudaud@ecoledubois.fr (C. Boudaud), jerome.humbert@gmail.com (J. Humbert), jbaroth@ujf-grenoble.fr (J. Baroth).

http://dx.doi.org/10.1016/j.engstruct.2014.10.053
0141-0296/

This refined FE model of shear wall, explained in details in Part I, is developed using beam elements for the frame, plate elements for the sheathing panel and two-node spring-like elements for the panel-to-frame and frame-to-frame joints. This 2D model is embedded at the location of the sill plate, and masses are uniformly distributed along the top plate. Except for Richard et al. and Judd, the aforementioned authors used their refined FE model to calibrate a simplified nonlinear force–displacement relationship under quasi-static loading and implemented this force–displacement behaviour into a structural model of a building. Then, the authors could predict the seismic response of a building and compare it with the results obtained by dynamic shake table tests. Richard et al. and Judd have validated their refined FE model by comparing their predictions to dynamic tests performed on a single specimen. The validation of refined FE models under dynamic loading is rarely conducted; a few studies can nevertheless be mentioned, such as Dolan [7], Yamaguchi et al. [26], Durham et al. [8], Richard et al. [20], and Varoglu et al. [24] who performed dynamic tests on shear walls. In the present study, dynamic shake table tests on shear walls are performed to observe the wall behaviour and to validate the refined FE model under such loading.

Once the refined FE model is fully validated using experimental quasi-static and dynamic tests, a simplified FE model can be developed. Indeed, refined FE models are time-consuming, which can be too restrictive for use at the scale of a complete structure, such as a multi-storey building. To address this issue, one alternative is to use simplified FE models. The behaviour of these models is defined by a limited number of degrees of freedom (DOFs). In the aforementioned studies [11,21,25,18,19], the simplified FE models were calibrated on refined FE model predictions. However, they can also be calibrated directly from experimental tests on shear walls [23,17,10,1,6,2]. Simplified FE models are calibrated on quasi-static force–displacement evolutions and used to perform dynamic calculations. However, to the best of our knowledge, this calibration has never been validated by comparing the dynamic behaviour of the refined and simplified FE models or by using experimental dynamic tests on a single shear wall. This validation step is emphasised in this paper. Finally, a method to build a wall by combining simplified FE models is described.

2. Refined FE model

2.1. Experimental dynamic tests

Dynamic tests were performed on a 6×6 m unidirectional shake table at the FCBA Technological Institute in Bordeaux, France. Two types of shear wall were tested. One was the P16 shear wall described in Part I, and the other specimen was similar to the OSB12 shear wall except for its nails, which were 2.5 mm in diameter and 55 mm in length. For the sake of comprehensiveness, the main characteristics of the shear walls are listed here: C24 strength class timber is used for the frame, the particleboard panel is 16 mm thick, the OSB panel is 12 mm thick, nail dimensions are 2.5×55 mm and the spacing is 150 mm on the panel edges and 300 mm in the middle, one reinforced bracket is used at the bottom of each of the two exterior studs. Fig. 1 shows the test facility. For such tests, the dead load can fall off onto the shake table if wall failure occurs, which is why Dolan [7] developed a moving frame that carries the load and transfers the inertial forces to the shear wall. Other studies have been performed using the same test apparatus [8,24], and Yamaguchi et al. [26] developed a moving frame made of a steel floor and two cross walls, which can test two shear walls simultaneously. For both apparatuses, the moving frame carries the dead load such that the shear wall is not submitted to a vertical load. Dolan added cables linking the top plate to the shake

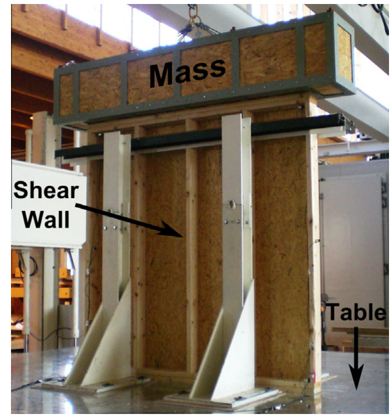

Fig. 1. Dynamic tests set-up on the shake table (FCBA Technological Institute).

table, to create a vertical load. Another type of system was used by Dutil and Symans [9], in their case, gravity loading was applied through a load beam attached to the top plate of the wall, and the out-of-plane instability was limited by means of rubber casters rolling on the load beam. Similar to Dutil and Symans, in the present study, it was decided to directly fix the mass (1500 or 2000 kg) onto the shear wall. For this purpose, a box was bolted to the top plate and filled with ballast. The out-of-plane instability is limited by means of a frictionless guiding system. This set-up ensured that the test conditions for the shear walls were similar to the *in situ* conditions. The anchorage of the shear walls was similar for dynamic and quasi-static tests; however, only 3D bracket-type connectors were used for exterior anchorage.

A total of 12 dynamic tests were performed (Table 1), based on different configurations (OSB12 or P16 shear wall), masses (1500 or 2000 kg), accelerograms (3 different accelerograms were used, each test using only one) and accelerogram scaling factors (accelerograms scaled to different PGA values). The first accelerogram is the natural l'Aquila earthquake accelerogram (April 2009), recorded at the GX066 station. It was selected because it represents a realistic signal for western Europe. The two others signals were selected to correspond to a more severe seismic hazard. The scenario for Guadeloupe (French Antilles) has been chosen. The most probable magnitude–distance couple was identified for this scenario and for a return period of 475 years (probability of exceedance of the peak ground acceleration of 10% in 50 years). Then, corresponding signals were found in all available databases. As a result, the El Salvador earthquake accelerogram (February 2001) recorded at the Zacatecoluca station was selected. The same procedure provided another accelerogram, which was then modified using the RSPMatch2005 [13], so that its spectra fits a calculated spectra. This calculated spectra was obtained with the Youngs et al. [28] relationship, which provides a more complete and realistic frequency content for the Guadeloupe scenario. This third accelerogram is referred to as Guadeloupe. Considering the high number of variables (shear wall types, masses, accelerograms and scaling factors), the number of tests is relatively low. For that reason, the effect of parameters could not be studied, and the analysis is limited to general observations. Fig. 2 presents the 5% damped pseudo-acceleration response spectra of the three unscaled motions.

Tests were performed using a train of motions, *i.e.* by repeating an accelerogram with increasing scaling ratios of the PGA. The goal of this procedure was to reach failure of the shear wall and provide information regarding the shear wall behaviour at different levels of loading. Before each accelerogram (including the first), a low amplitude white noise test was performed to measure the fundamental frequency of the shear wall. Fig. 3 presents the Frequency

Table 1
Shear walls configurations for dynamic tests.

Test	Panel	F2F angle	P2F	Mass	Accelerogram	
			($\varnothing \times L$)	kg	Name	PGA sequence (g)
1	OSB12	AH	2.5×50	1500	El Salvador	0.73–0.24–0.88
2					L'Aquila	1.3–0.56–1.8
3					Guadeloupe	0.33–1.06–0.33–1.25
4						0.33–1.06–0.33–1.25
5						0.33–1.06–0.33–1.25
6						1.06–0.33–1.25
7				2000	El Salvador	0.73–0.24–0.88
8					Guadeloupe	1.06–0.33–1.25
9	P16			1500	L'Aquila	1.8–0.56–1.8
10					Guadeloupe	0.33–0.66–1.25–0.33
11				2000	L'Aquila	0.56–1.8–0.56
12					Guadeloupe	0.33–1.25–0.33–1.25

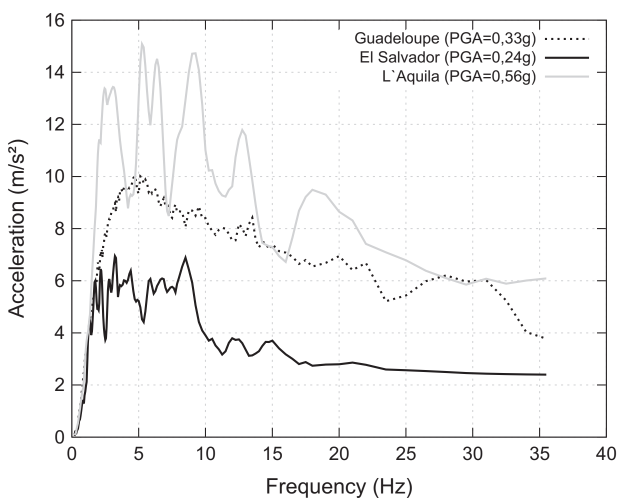

Fig. 2. 5% damped pseudo-acceleration response spectra of the three unscaled motions.

Response Function (FRF) for one test (OSB12 – 1500 kg – Guadeloupe). The undamaged specimen has a fundamental frequency of 6.25 Hz. After the first accelerogram (PGA = 0.33 g), the frequency decreased to 5.0 Hz. After the second accelerogram (PGA = 1.06 g), the fundamental frequency decreased even more (2.25 Hz). The third accelerogram (PGA = 0.33 g) did not appear to change the FRF, which was expected due to its low PGA compared with the second accelerogram. Because failure occurred during the fourth accelerogram (PGA = 1.25 g), no additional white noise analysis was achieved. The decrease in stiffness (20%) and amplification (40%) after the first loading, which can be interpreted as damages in the shear wall, are obvious on Fig. 3. Nevertheless, post test visual observations did not reveal any visual clue of that degradation. For the first loading, the relative displacement at the top of the wall was about 10 mm, which correspond to a small drift of 0.4%. Therefore, it is considered that the degradation of the wall behaviour is in fact due to small gaps appearing in the joints. For loadings resulting in greater displacements, post test observations show withdrawals (Fig. 4a) or pulling through (Fig. 4b) of the most loaded nails (in the corners of the sheathing panels). When the failure of the wall is reached, most of the nails joints correspond to the pictures of Fig. 4. One should note that the failure modes presented herein, that occur in a shear wall specimen under dynamic loading, are in accordance with the results of the tests on nail joints previously described (see Part I).

The damping ratio of the shear walls can also be estimated experimentally. It provides a global damping ratio that accounts for all energy dissipation phenomena under small relative displacements to avoid material non linearity (plasticity, damage). These measures were performed for a relative displacement of the wall of the order of 1 mm. Two calculation methods were used, the bandwidth method based on the FRF and the logarithmic decrement method based on the free vibration response. The results showed that the damping ratios ranged between 10% and 17% when calculated with the bandwidth method and between 6% and 9% for the logarithmic decrement method. The same discrepancies between the two methods were observed by Dutil and Symans [9], who concluded that the maximum amplitude of the FRF could not be known with sufficient precision to assure satisfactory results. Therefore, only the logarithmic decrement method is considered here.

All measurements were first recorded by accelerometers located in key positions (on the table to check the effective input signal; on the sill plate to check the current anchorage behaviour; on the exterior studs to check their possible uplift and bending; on the top plate to measure the wall deformation). Because this measurement system cannot account for the after-test permanent deformations due to the hysteretic behaviour of the shear wall, two displacement sensors were added. An LVDT transducer measured the absolute displacement of the shake table, and a draw-wire sensor measured the absolute displacement between the top plate of the specimen and the laboratory. The relative displacement of the shear wall was derived from these data.

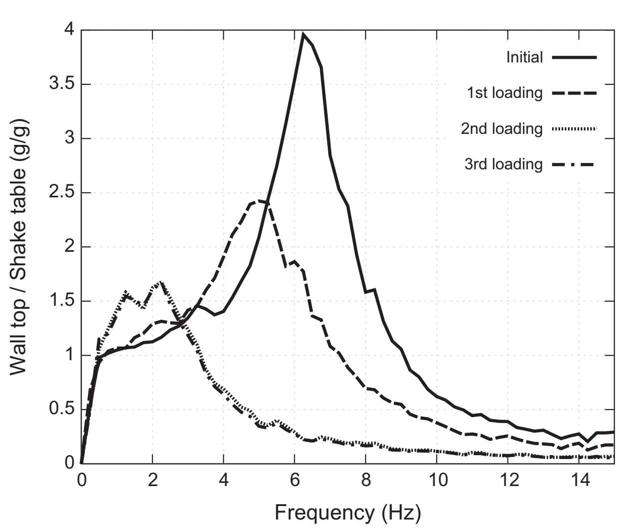

Fig. 3. Frequency Response Function (OSB12 – 1500 kg – Guadeloupe).

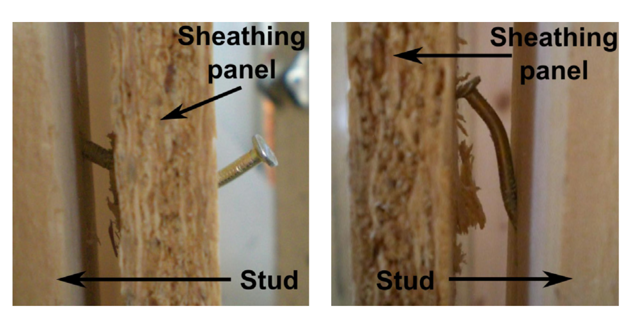

(a) Withdrawal (b) Pulling through

Fig. 4. Post test observations on the nail joints.

2.2. FE model for dynamic calculations

In Part I, the refined FE model for quasi-static calculations was presented. It was composed of beam elements that modelled the studs, sill, and top plate of the frame. The beam and panel elements exhibit linear, elastic behaviour and were connected by means of two-node, spring-like elements with a specific nonlinear hysteretic constitutive relation (see Part I) to model the joints with metal fasteners. The proposed constitutive behaviour law is versatile (valid for any type of metal fastener and any type of loading) and takes into account the cumulative damage. For each type of fastener, the model parameters were calibrated using the test results performed on the joints. For the tests, lumped masses were added to the wall's top plate to account for the roof weight and/or upper story (1500 or 2000 kg per shear wall). The weight of the shear wall was approximately 45 kg. The damping matrix was built with the Rayleigh method ($C = \alpha K + \beta M$), with α and β selected in order to have the same damping value at the first two vibration modes (with K the stiffness matrix and M the mass matrix).

The experimental results showed that the global damping ratio (ξ_{glob}) ranged between 6% and 9% for maximal relative displacements that did not exceed 1 mm. Assuming that the energy dissipation was concentrated in the metal fasteners, a viscous damping ratio (ξ_{visc}) was identified such that the addition of viscous damping dissipation and hysteretic dissipation for all the joints allows to correctly predict the free vibration of the wall for a maximal relative displacement of less than 1 mm. The identification led to $\xi_{visc} = 5\%$. This damping ratio was thus taken into account for each joint and for all calculations.

2.3. FE model validation under dynamic loading

The refined FE model of the shear wall was validated under quasi-static loading in Part I. To complete the validation of the refined FE model, dynamic calculations were performed and the results are compared with that of the experimental dynamic tests. Fig. 5 presents the experimental and predicted displacement–time evolutions for the P16 specimen with a mass of 1500 kg and the "Guadeloupe" accelerogram (PGA = 0.33–0.66–1.25 g).

The model predictions are generally in good agreement with the experimental results. For long simulated time (third accelerogram amplitude, more than 60 s), the model is less accurate, most likely

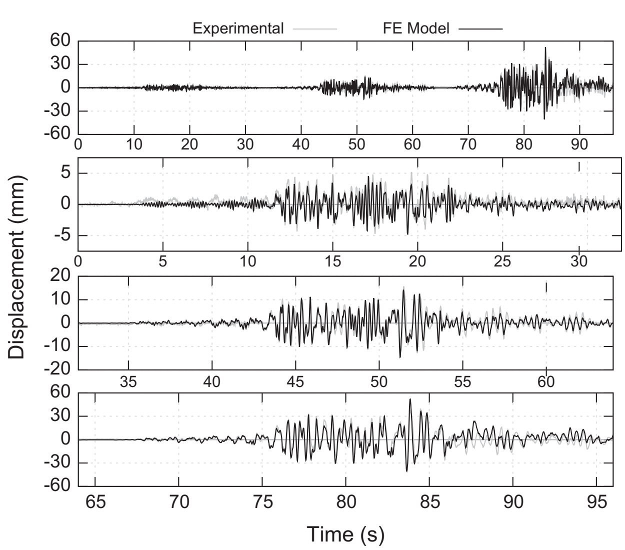

Fig. 5. Top displacement of shear wall: Comparison of experimental and numerical time evolution for test 10.

because of the specific loading protocol and the damage accumulation in the shear wall during the three sequential tests. Because real earthquakes do not last so long, the slight discrepancy between the experimental and predicted results is not considered an issue. The different configurations (shear wall specimen, mass, and accelerogram) result in a total of 12 dynamic tests, but only 11 could be used because of data acquisition issues for test number 12. For each test, the Fig. 6 presents the experimental and numerical peak displacements for the first loading on the specimen. It can be seen that the predictions are more accurate for some tests than others, but on the whole the model is able to predict the behaviour for different configurations of shear walls and different levels of loading. The experimental variability is difficult to assess, as each test is achieved on either a different configuration of shear wall or a different loading, except for tests 3, 4 and 5 which are identical (Table 1). Fig. 6 shows that for these tests (3, 4 and 5), the experimental results present a relative difference in terms of peak displacement. Moreover, the fundamental frequency is measured before each test and the values present a coefficient of variation of about 10%. Despite all the care given during each step of the experimental process, the reasons for this variability can be explained in various ways (materials, fabrication, storage, installation on the test machine, measurement accuracy, etc.). As the FE model is deterministic, it should be considered that a portion of the differences between experimental and numerical results can be explained by this experimental variability.

3. Simplified FE model

Modelling an entire 3D timber-framed structure on the scale of elementary components (joints) may lead to significant computational costs. Thus, a simplified FE model is proposed to model shear walls.

3.1. Simplified element development

Fig. 7 presents the proposed simplified FE model for shear walls. Various simplified FE models have been already proposed (e.g. Folz and Filiatrault [11], Richard et al. [21], Xu and Dolan [25], van de Lindt et al. [18], Pang and Rosowsky [19]), but we propose to use our own hysteretic constitutive law to build it. This simplified FE model is composed of a frame of bars, which ensures a parallelogram-like deformation. This is the dominant deformation for shear walls [12], but overturning due to uplift of the anchorages also exists. More complicated FE elements can be developed to account for it Christovasilis and Filiatrault [4,5]. Since the constitutive law that describes the behaviour of the simplified FE model is calibrated based on the refined FE model predictions (which reproduces both shearing and overturning deformation), the effect of the overturning is indirectly taken into account in the simplified FE model. This effect is primarily related to exterior anchorages, the mass at the top of the wall and the aspect ratio (height over length of the wall). In this work, the aspect ratio is not a parameter of the study, as only one geometry of shear wall (2400 × 2040 mm) is used. Experimental and numerical results showed insignificant uplift for reinforced 3D bracket-type connectors (AH®) regardless of the level of vertical loading (from 0 to 5000 kg). Because standard 3D bracket-type connectors (E5®) are less stiff than reinforced connectors, plastic strain of the 3D bracket-type connectors was observed, which lead to greater uplift values (up to 25 mm). However, such values are small compared to the dimensions of the wall (2400 × 2400 mm), which results in a limited impact on the overturning of the behaviour of the wall.

A two-node spring-like element controls the horizontal drift of the wall. The nonlinear behaviour of the simplified FE model arises

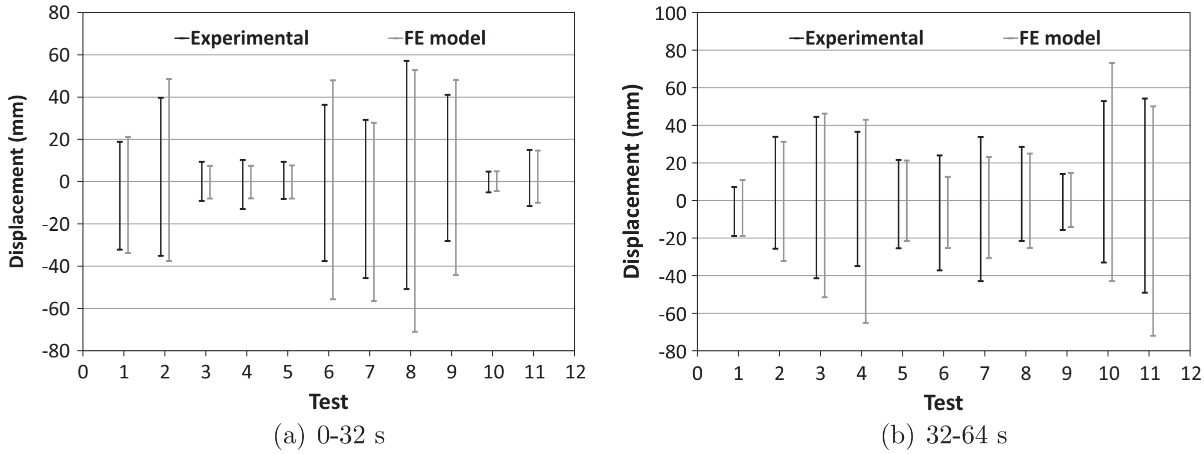

Fig. 6. Peak displacements comparison between experimental results and refined FE model predictions on each specimen.

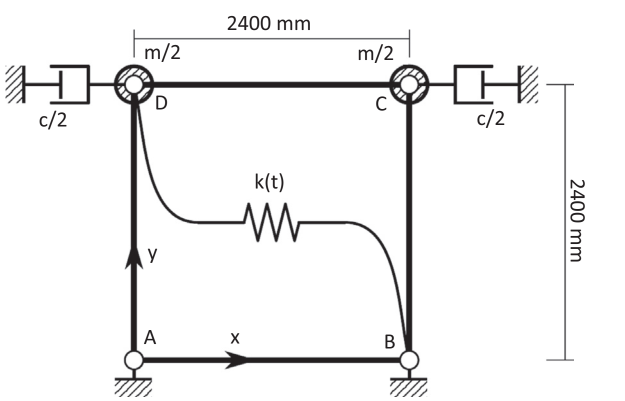

Fig. 7. Proposed simplified FE model composed of a rigid frame of bars ABCD, a spring-like element with nonlinear, semi-rigid behaviour $k(t)$, two lumped masses, $m/2$, that model the roof load and two dampers, $c/2$.

from the constitutive relationship used for the joints (see Part I). The parameters of this nonlinear model were identified from the results of the refined FE model under both push-over and cyclic loadings. Indeed, the objective of using simplified FE models is to prevent costly experimental tests on shear walls, replacing them with tests on joints only. In the present study, however, experimental tests on shear walls were performed but only for validation purposes. The roof load, which is predominant, is modelled with two lumped masses, $m/2$.

3.2. Simplified element calibration

The calibration process is similar to the direct calibration presented in Part I. The backbone parameters were calibrated using the refined FE model prediction under quasi-static, monotonic loading (Fig. 8). Then, pinching and damage parameters were identified by means of successive simulations used to best fit the refined FE model prediction under quasi-static, reversed cyclic loading (Fig. 9). This means that a detailed FE model has to be build for every configuration of simplified FE model. The detail of the parameters of the constitutive law can be found in Part I.

3.3. Simplified FE model validation

The simplified FE model was calibrated for quasi-static loading and then used in the dynamic calculations. To assess the accuracy of its behaviour under dynamic loading, the simplified FE model predictions and the experimental results under dynamic loading were compared, and those predictions were also compared with those of the refined FE model. The dynamic calculations performed on both the refined and the simplified models showed that the computation time ratio is approximately 12. Fig. 10 shows a global comparison in terms of peak displacements between experimental results, refined and simplified FE models predictions for the first loading (0–32 s, Fig. 10a) and second loading (0–32 s, Fig. 10b).

The results show that the simplified and the refined FE models match perfectly under quasi-static loading (see calibration, Fig. 9), whereas under dynamic loading, the model do not match as well. Considering the limited number of degrees of freedom, and the subsequent gain in computation time provided by the simplified FE model, the confrontations between experimental, refined FE model, and simplified FE model (Fig. 10) show a good agreement. Nevertheless, in an attempt to improve the simplified FE model, two other developments were tested:

- The initial stiffness parameter (K_0) directly affects the fundamental frequency of the simplified element. Because K_0 was calibrated using beginning points of the force–displacement evolution (Fig. 8), the fundamental frequency of the simplified model does not properly match the fundamental frequency of the refined FE model. Therefore, K_0 was modified to match the fundamental frequency of the refined FE model (*e.g.*, 3.9 Hz for the P16 specimen with E5 connectors).
- The lumped masses used in the simplified model do not take into account the weight of the shear wall itself. Though this weight is relatively small ($\simeq$ 50 kg) compared with the mass

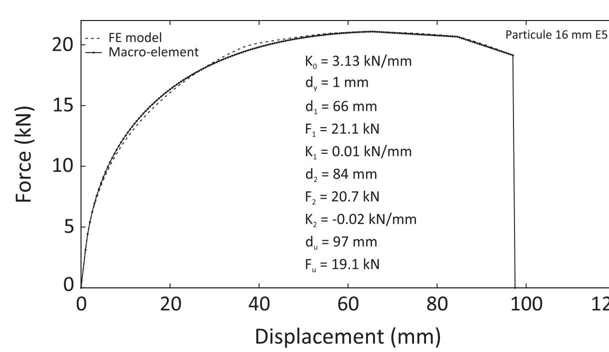

Fig. 8. Step 1: Calibration of backbone parameters using the prediction of the shear wall response under quasi-static loading: P16 panels and E5 connectors.

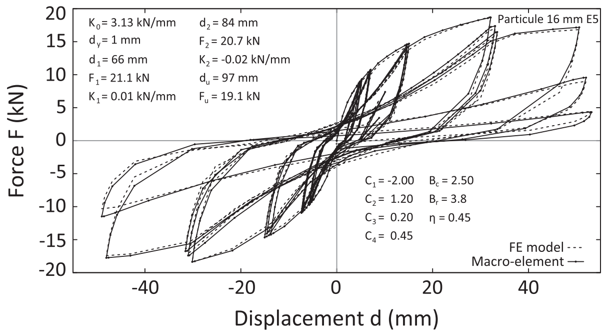

Fig. 9. Step 2: Calibration of pinching parameters using the prediction of the shear wall response under quasi-static, reversed cyclic loading: P16 panels and E5 connectors.

applied to the top of the wall (1500 or 2000 kg), it is nevertheless taken into account in the refined model. Therefore, the mass of the wall is modelled by adding equally distributed lumped masses on the four nodes of the simplified FE model.

Calculations with and without these improvements showed that their effect is limited and sometimes insignificant, which, in retrospective, can be explained by the fact that the modifications are of really slight amplitude (50 kg represent only 3% of 1500 kg), and the order of magnitude does not exceed 5% for the modification of the initial stiffness. However, the models were coded as described, and the results presented in Fig. 10 were obtained with the improved simplified model.

3.4. Use of the simplified FE model

The simplified FE model was developed to build accurate and computationally time efficient models of buildings. An entire 3D building model can be obtained by connecting different simplified FE models. One of the calculation methods of Eurocode 5 [3] for the shear wall racking resistance does not consider the parts with openings. As discussed by Yasumura [27], and Silih et al. [22], their influence is far from insignificant ([15] also provides a calculation method for perforated shear walls), therefore openings areas of shear walls are studied in this work. They can be modelled either by a simplified FE model that includes adjacent shear walls or by

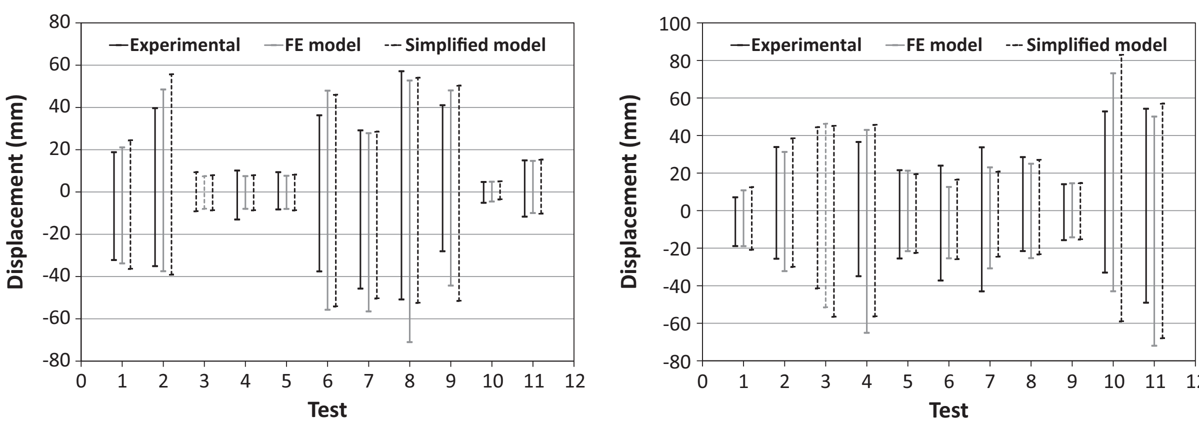

(a) 0-32 s (b) 32-64 s

Fig. 10. Peak displacements comparison between experimental results, refined and simplified FE models predictions on each specimen.

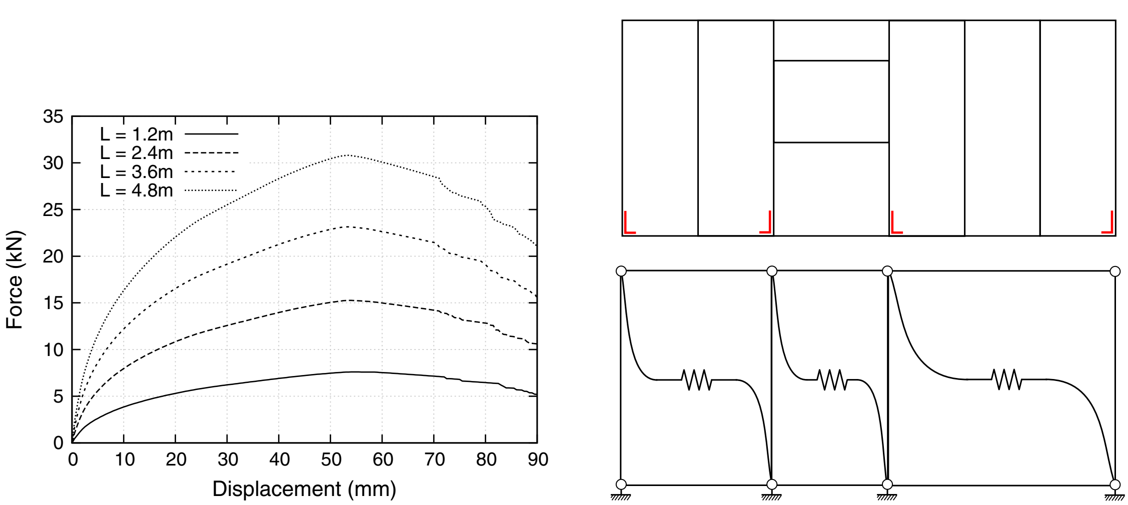

(a) Force–displacement evolutions for different shear wall lengths

(b) Discretisation of a wall into simplified elements

Fig. 11. Modelling of walls by simplified elements.

a specific simplified FE model limited to the opening area. The latter is proposed in this study for the following reasons:

- Fig. 11a presents the force–displacement evolutions of shear walls of different lengths (calculate with the refined FE model) and shows that the maximal force is proportional to the length of the wall. Due to this property, the number of necessary refined FE models required to calibrate the simplified models is reduced to one. This property is only valid for blind shear walls (without openings).
- Fig. 11b shows an example of a discretisation of a wall into simplified elements. The two full shear walls were modelled by simplified elements, which were calibrated using a unique, refined FE model. The opening area was modelled by a specific simplified element, which requires a refined FE model for its calibration. Yet, due to the opening and the relatively small dimensions of the simplified element, the refined FE model is relatively computationally light and therefore, can be quickly developed and calculated.

4. Conclusions

This paper (along with Part I) presents refined and simplified FE models of a timber-framed shear wall under seismic loading. The refined FE model showed good agreement with 14 experimental tests for quasi-static loading in Part I. In this part, the refined FE model was used to perform dynamic calculations. The results are compared with 11 experimental tests under seismic loadings. The refined FE model predictions are in good agreement with the experimental data under seismic loading. To reduce the calculation time for dynamic simulations, a simplified FE model was developed. The calibration of this element was based on the refined FE model results under quasi-static loadings. The results obtained with the two models for dynamic calculations were compared. The results were reasonably close, and the simplified model provides a significant advantage in calculation time. The discretisation of a wall into several simplified elements is based on the property of proportionality between the maximal force of a full shear wall and its length. The main features of this work are:

- The use of a versatile constitutive law able to model the dissipative behaviour of different types of joints.
- Its calibration on an important number of joint tests, allowing to take into account the variability of the joints mechanical behaviour.
- The development of a refined FE model of shear walls corresponding to common building practice in Western Europe.
- The confrontation of this model predictions to a more important number of experimental tests (under both quasi-static and dynamic loadings) than currently found in the literature.
- The development of a simplified FE model of shear wall aiming at reducing the computational time for nonlinear dynamic calculations.
- Its calibration based on predictions of the refined FE model under quasi-static loading, and its validation under dynamic loading, which is to the best of our knowledge not studied in the literature.
- The definition of an efficient method, based on verified shear walls mechanical properties, to build the walls of a timber-framed building by coupling simplified FE models.

In the future, the development of FE models of a complete buildings will be studied. In the case of a building with several storeys, the simplified model of shear wall should be able to account for the overturning phenomenon (the refined model already can). In the case of a single storey structure, the main outlook of this work is obviously the development of a FE model and its confrontation to experimental data, which is currently ongoing research.

Acknowledgements

The SISBAT research project is funded by the French Agency ANR (Agence Nationale de la Recherche ANR-08-RISKNAT2008). Authors would like to express their gratitude for this support and thank the members of this project for their contributions and databases, especially Mrs C. Faye (FCBA Technological Institute) and her colleagues, for the effort provided.

References

[1] Ceccotti A, Karacabeyli E. Validation of seismic design parameters for wood-frame shear wall systems. Can J Civ Eng 2002;29:484–98.
[2] Ceccotti A, Sandhaas C. A proposal for a standard procedure to establish the seismic behaviour factor q of timber buildings. In: World conference on timber engineering proceedings; 2010.
[3] CEN. EN 1995-1-1: design of timber structures. Part 1-1 : General – common rules and rules for buildings; 2005.
[4] Christovasilis I, Filiatrault A. Two-dimensional numerical framework for the nonlinear static and dynamic analysis of light-frame wood structures. In: Proc world conference on timber engineering; 2010.
[5] Christovasilis I, Filiatrault A. Numerical and experimental investigation of the seismic response of light-frame wood structures. MCEER technical report 11-0001 multidisciplinary center for earthquake engineering; 2011.
[6] Collins M, Kasal B, Paevere P, Foliente G. Three-dimensional model of light frame wood building. I: Model description. J Struct Eng 2005;131(4):676–83.
[7] Dolan J. The dynamic response of timber shear walls. Ph.D. thesis. University of British Columbia, Vancouver (BC, Canada); 1989.
[8] Durham J, Lam F, Prion H. Seismic resistance of wood shear walls with large osb panels. J Struct Eng 2001;127(12):1460–6.
[9] Dutil D, Symans M. Experimental investigation of seismic behavior of light-framed wood shear walls with supplemental energy dissipation. In: Proc 13th world conference on earthquake engineering. Paper no. 3421; 2004.
[10] Foliente G. Hysteresis modeling of wood joints and structural systems. J Struct Eng 1995;121:1013–22.
[11] Folz B, Filiatrault A. Cyclic analysis of wood shear walls. J Struct Eng 2001;127(4):433–41.
[12] Gupta A, Kuo G. Behavior wood-framed shear walls. J Struct Eng 1985;111(8):1722–33.
[13] Hancock J, Bommer J, Stafford R. Numbers of scaled and matched accelerograms required for inelastic dynamic analyses. Earthq Eng Struct Dyn 2006;37:1585–607.
[14] He M, Lam F, Foschi R. Numerical analysis of statically loaded three-dimensional timber light-frame buildings. In: Procedings of the world conference on timber engineering, Whistler, British Columbia, Canada; 2000.
[15] ICC. International building code; 2000.
[16] Judd J. Analytical modeling of wood-frame shear walls and diaphragms. Master's thesis. Brigham Young University; 2005.
[17] Kasal B, Leichti R, Itani R. Nonlinear finite element model of complete light-frame wood structures. J Struct Eng 1994;120(1):100–19.
[18] van de Lindt J, Pei S, Liu H, Filiatrault A. Three-dimensional seismic response of a full-scale light-frame wood building: numerical study. J Struct Eng 2010;136(1):56–65.
[19] Pang W, Rosowsky D. Beam-spring model for timber diaphragm and shear walls. Struct Build 2010;163(SB4):227–44.
[20] Richard N, Daudeville L, Prion H, Lam F. Timber shear walls with large openings: experimental and numerical prediction of the structural behaviour. Can J Civ Eng 2002;29:713–24.
[21] Richard N, Yasumura M, Davenne L. Prediction of seismic behavior of wood-framed shear walls with openings by pseudodynamic test and fe model. J Wood Sci 2003;49:145–51.
[22] Silih E, Premrov M, Silih S. Numerical analysis of timber-framed walll elements coated with single fibre-plaster boards. Eng Struct 2003;41:118–25.
[23] Stewart W. The seismic design of plywood-sheathed shear walls. Ph.D. thesis. Univ. of Canterbury, Christchurch, New Zealand; 1987.
[24] Varoglu E, Karacabeyli E, Stiemer S, Ni C, Buitelaaar M, Lungu D. Midply wood shear wall system: performance in dynamic testing. J Struct Eng 2007;133(7):1035–42.
[25] Xu J, Dolan J. Development of a nailed wood joint element in abaqus. J Struct Eng 2009;135(8):968–76.
[26] Yamaguchi N, Karacabeyli E, Minowa C, Kawai N, Nakamura I. Seismic performance of nailed wood-frame shear walls. In: Proceedings of the world conference on earthquake engineering; 2000. N 877.6.A.
[27] Yasumura M. Racking resistance of panel-sheathed shear walls with openings. In: Proceedings of the 11th world conference on timber engineering; 2010.
[28] Youngs RR, Chiou S-J, Silva WJ, Humphrey JR. Strong ground motion attenuation relationships for subduction zone earthquakes. Seismol Res Lett 1997;68(1):53–73.